Intranuclear-Cascade Calculation of the Secondary Nucleon Spectra from Nucleon-Nucleus Interactions in the Energy Range 340 to 2900 MeV and Comparisons with Experiment*

HUGO W. BERTINI
Oak Ridge National Laboratory, Oak Ridge, Tennessee 37830

(Received 21 March 1969; revised manuscript received 8 September 1969)

Total nonelastic cross sections and the nucleon spectra fron continuum-state transitions for protons on complex nuclei are calculated using the intranuclear-cascade approach. Comparisons with experiment are made over the energy range 340–2900 MeV. The diffuseness of the nuclear surface, the energy distribution of the bound nucleons, and the exclusion principle are taken into account in the model of the nucleus, while experimentally determined free-particle elastic, inelastic, and differential cross sections are utilized in the calculation of the particle-particle reactions assumed to take place inside the nucleus. The Sternheimer-Lindenbaum isobar model is used in describing all pion-production processes. All but two of the comparisons with experiment are made on an absolute basis. The theoretical nonelastic cross sections and the theoretical secondary-particle spectra resulting from continuum-state transitions are shown to be in reasonable agreement with experimental data over the broad energy range considered. The effect of pion production and the effect of the diffuse nuclear boundary are illustrated for a few cases. The quasifree peak is shown to be dominated by single-scattering events that take place inside the nucleus.

INTRODUCTION

It has been shown[1–3] that a reasonable description of nuclear reactions involving nucleons incident on complex nuclei in the energy region below about 350 MeV can be obtained by assuming that the reaction proceeds initially by a fast cascade followed by a slower evaporation. The reactions considered are those leading to the continuum states of the nucleus. The present work is an extension to the 2-GeV energy region of these calculations.[2] An earlier calculation[4] in this energy region suffered from the lack of an adequate model in describing the pion-production processes that are assumed to take place within the nucleus during the particle-particle or cascade phase. It also suffered from the assumption that the nucleus was a sphere of uniform density. To a large extent, these deficiencies have been overcome in the present calculation, where the pion-production model used was the reasonably successful Sternheimer-Lindenbaum[5] isobar model, and where the nucleon density distribution was made to approximate the charge distribution obtained from electron scattering experiments.[6] The production reactions that are accounted for are single- and double-pion production in nucleon-nucleon collisions, and single-pion production in pion-nucleon collisions. The Monte Carlo method was employed in performing the calculation.

Comparisons between the theoretical secondary nucleon spectra and experimental data are made in subsequent sections. Experimental data for such comparisons were lacking at the time the earlier calculations were made.

NUCLEAR MODEL

The nuclear model is described in detail in Ref. 2. In summary, the nucleus was assumed to consist of three concentric spheres: a central sphere and two surrounding spherical annuli, each with a uniform density of neutrons and protons. The region boundaries were taken to be the same for the neutrons and protons. The proton density in each region was made to be proportional to the average value (over the same nuclear region) of the continuous Fermi-type charge distribution obtained by Hofstadter.[6] The neutron density in each region was set equal to the product of the proton density in the region multiplied by the neutron-to-proton ratio in the nucleus. There is, then, a three-region approximation to the continuously changing density distribution of nuclear matter within nuclei.

TABLE I. The backward fraction of neutron-proton elastic scattering as a function of energy.

Energy (MeV)	Fraction of total scattering with $\theta > \frac{1}{2}\pi$
600	0.47
800	0.46
930	0.44
1000	0.43
1500	0.37
2240	0.27
2750	0.21
4400	0.16

* Research partially funded by the National Aeronautics and Space Administration, Order No. H-38280A, under Union Carbide Corporation's contract with the U. S. Atomic Energy Commission.

[1] N. Metropolis *et al.*, Phys. Rev. **110**, 185 (1958).
[2] Hugo W. Bertini, Phys. Rev. **131**, 1801 (1963); **138**, AB2 (1965).
[3] K. Chen *et al.*, Phys. Rev. **166**, 949 (1968).
[4] N. Metropolis *et al.*, Phys. Rev. **110**, 204 (1958).
[5] R. M. Sternheimer and S. J. Lindenbaum, Phys. Rev. **123**, 333 (1961); **109**, 1723 (1958); **105**, 1874 (1957).
[6] R. Hofstadter, Rev. Mod. Phys. **28**, 214 (1956).

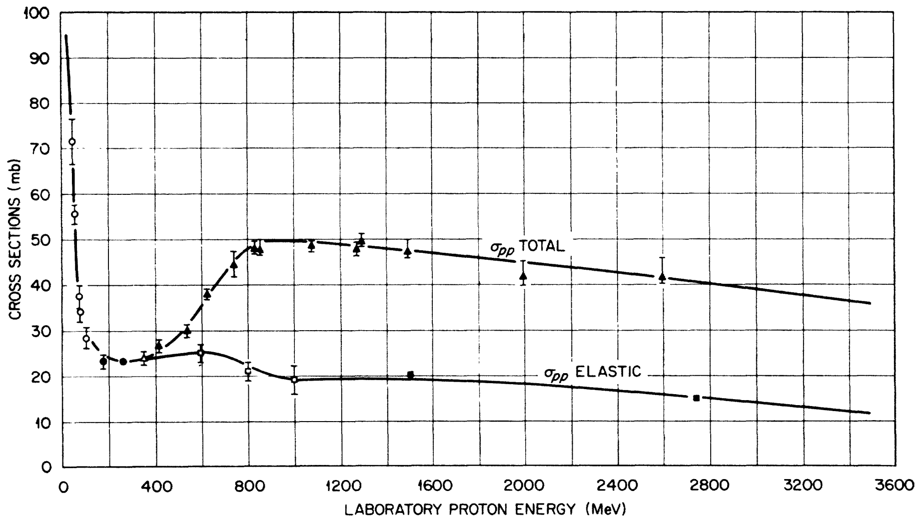

FIG. 1. Proton-proton total and elastic cross sections versus energy. ○, U. E. Kruse, J. M. Teem, and N. F. Ramsey, Phys. Rev. **101,** 1079 (1956); ●, O. Chamberlain and J. D. Garrison, *ibid.* **95,** 1349 L (1954); △, O. Chamberlain, E. Segré, and C. Wiegand, *ibid.* **83,** 923 (1951); ▲, F. F. Chen, C. P. Leavitt, and A. M. Shapiro, *ibid.* **103,** 211 (1956); □, L. W. Smith, A. W. McReynolds, and G. Snow, *ibid.* **97,** 1186 (1955); ■, W. B. Fowler *et al., ibid.* **103,** 1479 (1956).

The neutrons and protons in the nucleus were assumed to have a zero-temperature Fermi energy distribution. Hence, their kinetic energies range from zero to the zero-temperature Fermi energies that were calculated from the density of protons and neutrons in each region. To account for the nuclear forces and to confine the nucleons that make up the nucleus to the nuclear volume, single-particle negative potentials were assumed to apply separately to the neutrons and protons in each region. The potential well depth for the protons was taken to be 7 MeV greater than the zero-temperature Fermi energy of the protons in each region. The well depth of the neutrons in each region was calculated in an analogous manner. The 7 MeV corresponds to the binding energy of the most loosely bound nucleon, and this applies to both neutrons and protons and is taken to be the same for all nuclei.

PARTICLE-PARTICLE CROSS-SECTION DATA

Nucleon-Nucleon Reactions

The proton-proton and neutron-proton scattering cross sections that were used in the calculation are shown in Figs. 1 and 2, and the proton-proton and neutron-

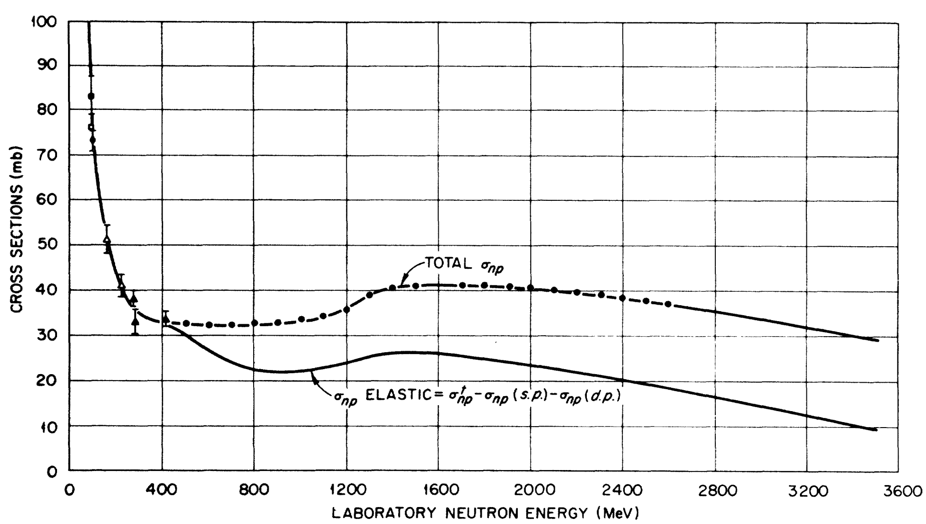

FIG. 2. Neutron-proton total and elastic cross sections versus energy. ■, L. J. Cook *et al.*, Phys. Rev. **75,** 7 (1949); □, J. Hadley *et al., ibid.* **75,** 351 (1949); ▼, J. DeJuren and N. Knable, *ibid.* **77,** 606 (1950); Δ, J. DeJuren and B. J. Moyer, *ibid.* **81,** 919 (1951); ▲, V. A. Nedzel, *ibid.* **94,** 174 (1954); ●, F. F. Chen *et al., ibid.* **103,** 211 (1956).

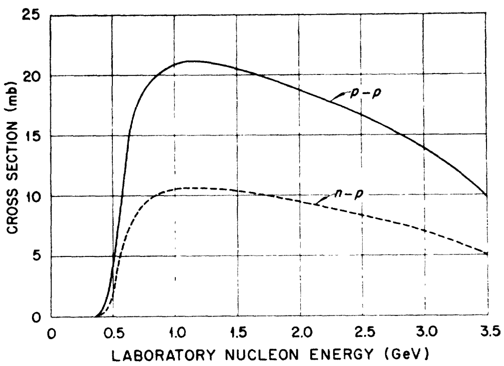

FIG. 3. Single-pion-production cross sections for p-p and n-p collisions. The p-p curve was obtained from data quoted by W. J. Fickinger *et al.* [Phys. Rev. **125**, 2082 (1962)] and the calculation of the n-p curve is described in the text.

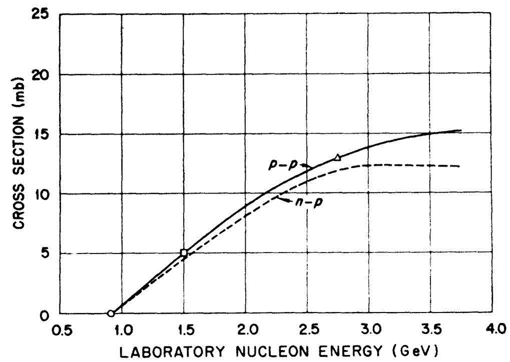

FIG. 4. Proton-proton and neutron-proton double-pion-production cross sections. ○, I. S. Hughes *et al.*, Phil. Mag. **2**, 215 (1957); □, W. B. Fowler *et al.*, Phys. Rev. **103**, 1479 (1956); Δ, F. F. Chen, C. P. Leavitt, and A. M. Shapiro, *ibid.* **103**, 211 (1956). The calculation of the neutron-proton double-production cross section is described in the text.

proton single-pion-production cross sections used are shown in Fig. 3. The n-p cross sections were taken to be half the p-p values, as is indicated by isotopic spin considerations when it is assumed that production occurs only through the formation of the $\frac{3}{2}$, $\frac{3}{2}$ isobar. The double-pion production cross sections for p-p and n-p reactions are shown in Fig. 4. The n-p cross section was calculated from the p-p cross section using the equation

$$\sigma_{n\text{-}p}{}^{\text{d.p.}}=\tfrac{1}{2}(\sigma_{p\text{-}p}{}^{\text{d.p.}})\{[\sigma(T=0)/\sigma(T=1)]+1\},$$

where the superscripts d.p. imply double-pion production, the σ's are the total cross sections, and the T's are the isotopic spins. The ratio of the cross sections in brackets was calculated from the total p-p and n-p cross sections (Figs. 1 and 2). It was explicitly assumed that this ratio is the same for the double-pion-production reactions.

Although it is likely that triple-pion-production events become important in the 2- to 3-GeV energy region, indications[7] are that at 2 GeV, the triple-production cross section is probably a factor of 5 smaller than the double-production cross section. Hence, the neglect of the triple-production cross section should not affect the bulk of the results presented here.

The low-energy p-p and n-p scattering cross sections are the same as those described in Ref. 2.

The p-p differential scattering cross sections below 1 GeV and the n-p differential cross sections below 740 MeV are those used in the previous work.[2] At higher energies, the shape of the n-p differential cross section in the forward and backward directions was arbitrarily taken to be equal to the shape of the p-p cross section, except that the fraction of the scattering directed into the backward hemisphere in the c.m. system as a function of energy was taken to be that shown in Table I. These values were obtained by an extrapolation to higher energies of the values calculated from the lower-energy data. The higher-energy p-p differential cross sections were taken from the papers in Ref. 8. In all scattering and production reactions, linear interpolation was used to obtain the cross section at any energy from the data that were tabulated at specific energies.

TABLE II. Ratio of average number of cascade neutrons to average number of cascade protons.

Case	Metropolis *et al.*[a]	Same nucleus as Metropolis *et al.*, different π-production model	Different nucleus, different model
690-MeV protons on Cu	1.02	1.37±0.03[b]	1.19±0.03[b]
1840-MeV protons on Al	0.92	1.1±0.03	1.0±0.02

[a] Reference 4.
[b] Calculated for 660-MeV protons.

TABLE III. Average number of emitted cascade nucleons per inelastic event.

Case	Metropolis *et al.*[a]	Same nucleus as metropolis *et al.*, different π-production model	Different nucleus, different model
690-MeV protons on Cr	4.3	4.7±0.03[b]	4.1±0.02[b]
1840-MeV protons	6.7	6.8±0.05	5.2±0.04

[a] Reference 4.
[b] Calculated for 660-MeV protons.

[7] D. V. Bugg *et al.*, Phys. Rev. **146**, 980 (1966).

[8] W. N. Hess, Rev. Mod. Phys. **30**, 368 (1958); J. D. Dowell *et al.*, Proc. Phys. Soc. (London) **74**, 625 (1959); Nuovo Cimento **18**, 818 (1960); W. B. Fowler *et al.*, Phys. Rev. **103**, 1489 (1956).

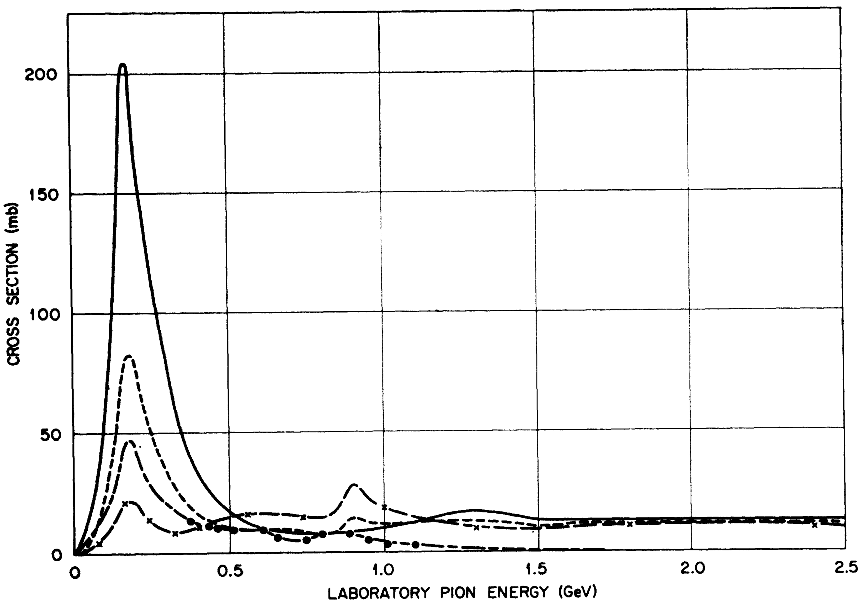

FIG. 5. Elastic pion-proton cross sections. Solid line, $\pi^+ + p$; dashed line, $\pi^0 + p$; line through x's, $\pi^- + p$; dot-dashed line, $\pi^- + p$ exchange; experimental points, P. Falk-Vairant and G. Valladas, Rev. Mod. Phys. **33**, 362 (1961). The calculations of the cross sections that are not measured directly are described in the text.

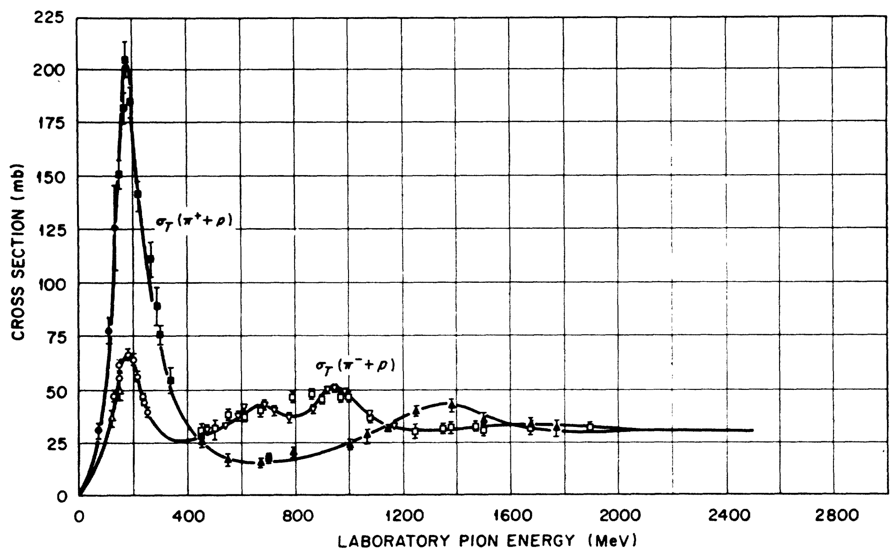

FIG. 6. $\pi^+ + p$ and $\pi^- + p$ total cross sections versus energy. ●, △, H. L. Anderson *et al.*, Phys. Rev. **91**, 155 (1953); ■, S. J. Lindenbaum and L. C. L. Yuan, *ibid.* **100**, 306 (1955); ▲, □, R. Cool, O. Piccioni, and D. Clark, *ibid.* **103**, 1082 (1956); ○, J. Ashkin *et al.*, *ibid.* **96**, 1104 (1954); ▽, H. C. Burrowes *et al.*, Phys. Rev. Letters **2**, 119 (1959).

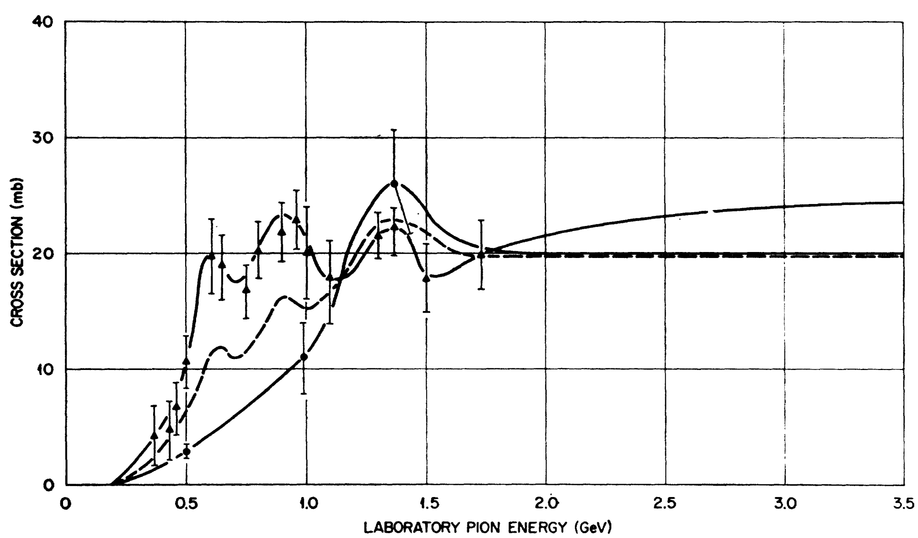

FIG. 7. Inelastic pion-proton cross sections. ▲, $\pi^+ + p$, and ●, $\pi^- + p$ from P. Falk-Vairant and G. Valladas, Rev. Mod. Phys. **33**, 362 (1961). The dashed line represents the $\pi^0 + p$ inelastic cross section, and its calculation is described in the text.

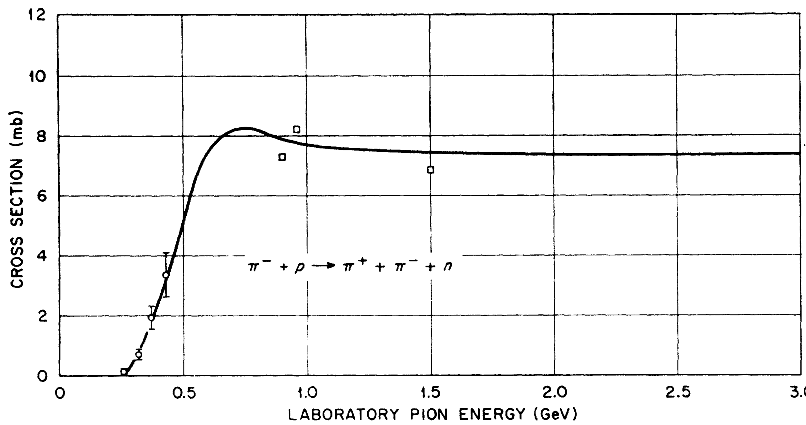

FIG. 8. The cross section for the $\pi^-+p\rightarrow\pi^++\pi^-+n$ reaction. ○, W. A. Perkins *et al.*, Phys. Rev. **118**, 1364 (1960); □, in *The Proceedings of the Sixth Annual Rochester Conference, On High-Energy Physics*, J. Ballam *et al.* (Interscience Publishers, Inc., New York, 1956), p. IV-16.

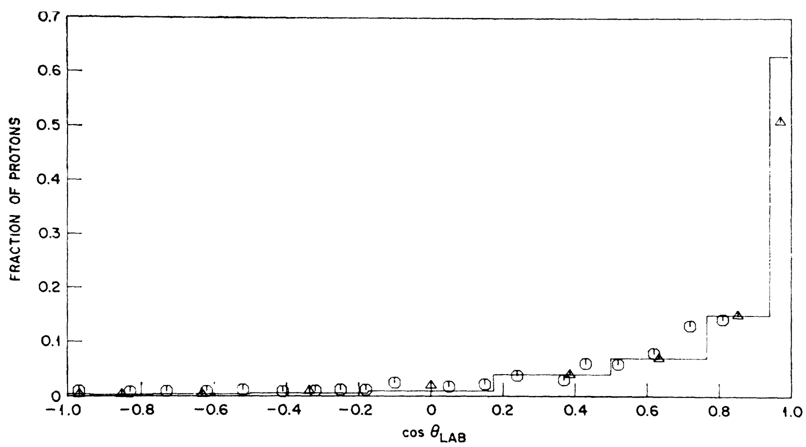

FIG. 9. Calculated angular distribution of protons emitted with energies greater than 90 MeV for 1840-MeV protons on aluminum. ○: Metropolis *et al.* (Ref. 4); △: same nuclear dimensions and density as Metropolis *et al.* (Ref. 1), but using isobar pion-production model; histogram: using diffuse nuclear surface and isobar model.

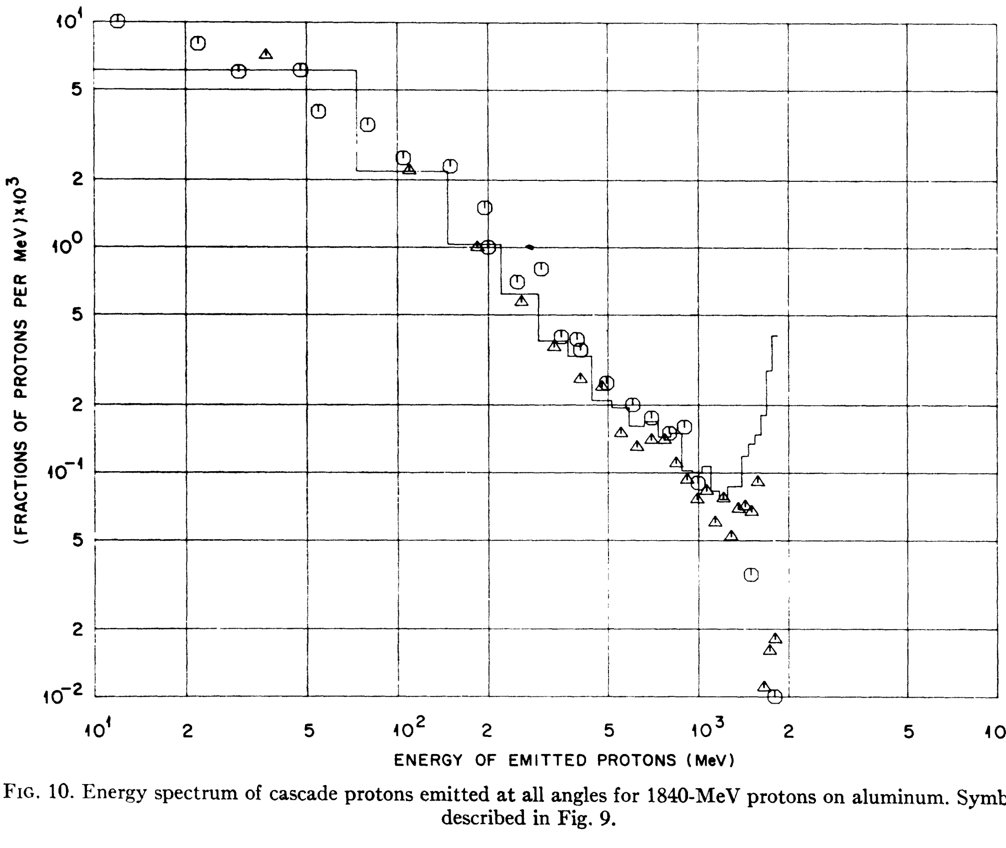

FIG. 10. Energy spectrum of cascade protons emitted at all angles for 1840-MeV protons on aluminum. Symbols described in Fig. 9.

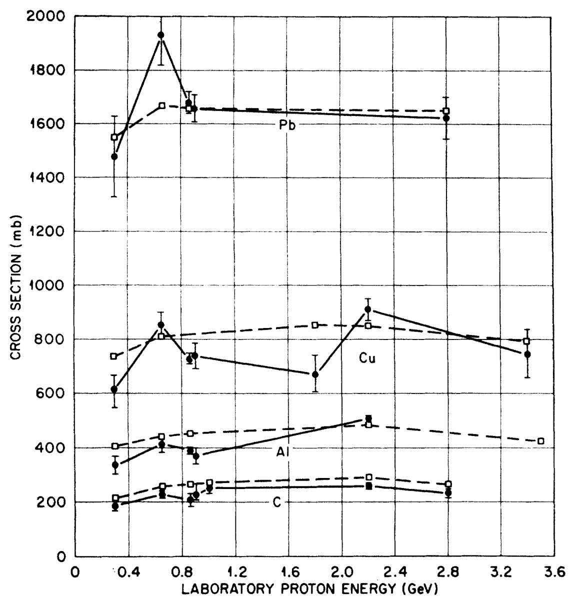

FIG. 11. Theoretical and experimental proton-nucleus inelastic cross sections versus proton energy. Straight lines are drawn between the points merely to guide the eye. □: theoretical values. The vertical dimensions of the open squares represent approximately two standard deviations. Points at 305 MeV: experimental data quoted by G. P. Millburn *et al.*, Phys. Rev. **95**, 1268 (1954); points at 650 MeV: experimental results of V. I. Moskalev and B. V. Gavrilovskii, Dokl. Akad. Nauk SSSR **110**, 972 (1956) [English transl.: Soviet Phys.—Doklady **1**, 607 (1956)]; points at 860 MeV: F. F. Chen *et al.*, Phys. Rev. **99**, 857 (1955); points at 900 MeV: N. E. Booth *et al.*, Proc. Phys. Soc. (London) **A70**, 209 (1957); point at 1000 MeV: G. J. Igo *et al.*, Nucl. Phys. **B3**, 181 (1967); point at 1.8 GeV: N. M. Kocharian *et al.*, Dokl. Akad. Nauk SSSR **107**, 668 (1956) [English transl.: Soviet Phys.—Doklady **1**, 209 (1956)]; points at 2.2 GeV: M. J. Longo and B. J. Moyer, Phys. Rev. **125**, 701 (1962); points at 2.8 GeV: T. Bowen *et al.*, Nuovo Cimento **9**, 908 (1958); point at 3.4 GeV: N. M. Kocharian *et al.*, Dokl. Akad. Nauk SSSR **107**, 668 (1956) [English transl.: Soviet Phys.—Doklady **1**, 209 (1956)].

Pion-Nucleon Reactions

The $\pi^+ + p$, $\pi^- + p$, and $\pi^0 + p$ scattering cross sections and the $\pi^- + p$ charge-exchange cross sections that were used are shown in Fig. 5. The $\pi^+ + p$ scattering cross section was calculated by subtracting the inelastic cross section (Fig. 7) from the total cross section (Fig. 6). The $\pi^- + p$ scattering and charge-exchange cross sections at energies below 340 MeV are the same as those used in the earlier work.[2] At higher energies, the cross sections reported in Ref. 9 were used. The elastic $\pi^0 + p$ cross section at energies greater than 320 MeV was calculated from the relation

$$\sigma_{\mathrm{el}}(\pi^0+p) = \tfrac{1}{2}[\sigma_{\mathrm{el}}(\pi^+ + p) + \sigma_{\mathrm{el}}(\pi^- + p) - \sigma_{\mathrm{ex}}(\pi^- + p)],$$

which is derived from the isotopic spin formalism. At energies below 320 MeV, the cross sections were taken to be those calculated in Ref. 2. The $\pi^0 + n$ cross section was set equal to the $\pi^0 + p$ cross section. This equality is dictated by the conservation of isotopic spin as are those equalities involving reactions of pions and nucleons whose charge states are the conjugates of those already described.

All inelastic pion-nucleon reactions were assumed to be single-pion-production events. The $\pi^0 + p$ inelastic cross section was calculated from the expression

$$\sigma_{\mathrm{inel}}(\pi^0 + p) = \tfrac{2}{3}\sigma_{\mathrm{inel}}(T=\tfrac{3}{2}) + \tfrac{1}{3}\sigma_{\mathrm{inel}}(T=\tfrac{1}{2}).$$

The inelastic isotopic spin $T=\frac{3}{2}$ and $\frac{1}{2}$ cross sections were taken from Falk-Vairant and Valladas.[9] The inelastic cross sections of the remaining charge states of the π-nucleon system were deduced from isotopic spin conservation.

The π-neucleon differential cross sections for energies below 340 MeV were the same as those used previously.[2] Above this energy, the cross sections were all set equal[10]

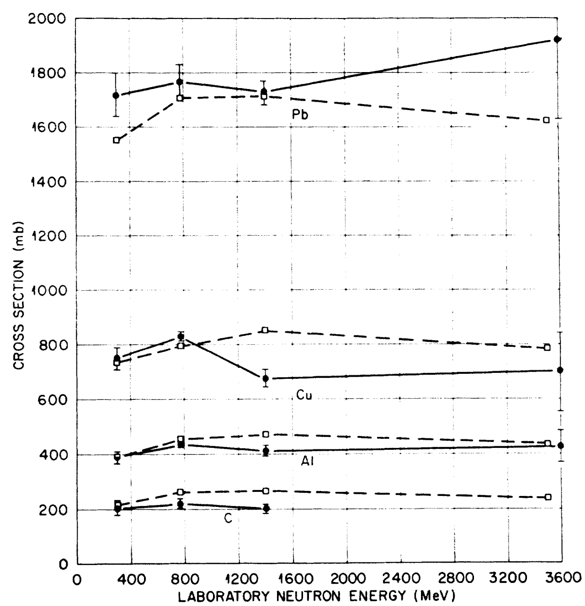

FIG. 12. Theoretical and experimental neutron-nucleus inelastic cross sections versus neutron energy. Straight lines are drawn between the points to guide the eye. □: theoretical values. The vertical dimensions of the squares represent about two standard deviations. Points at 300 MeV: experimental values quoted by G. P. Millburn *et al.*, Phys. Rev. **95**, 1268 (1954); points at 765 MeV: N. E. Booth *et al.*, Proc. Phys. Soc. (London) **71**, 293 (1958); points at 1.4 GeV: T. Coor *et al.*, Phys. Rev. **98**, 1369 (1955); points at 3.6 GeV: Paul H. Barrett, *ibid.* **114**, 1374 (1959).

[9] P. Falk-Vairant and G. Valladas, Rev. Mod. Phys. **33**, 362 (1961)].

[10] There is a much greater volume of pion-nucleon cross-section data available now than there was at the time the cross sections were incorporated into this program. The new cross sections are being processed for use, but it will be some time before that job is completed. The inaccuracies in the pion-nucleon differential cross sections should not greatly affect the data in this paper, which involve the secondary-nucleon spectra from incident nucleons.

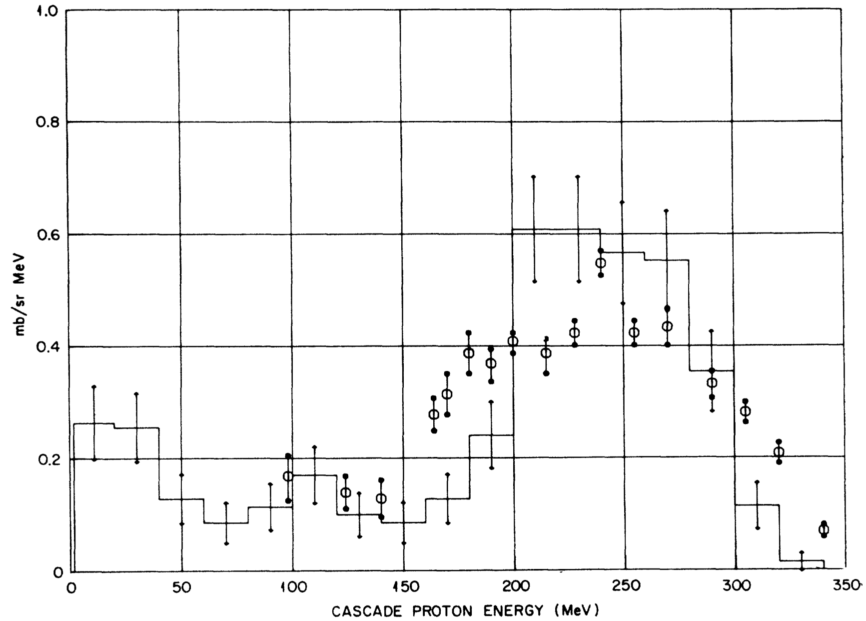

FIG. 13. Energy spectrum of cascade protons emitted at a laboratory angle of 30° from 340-MeV protons on carbon. Histogram: calculated values for the angular interval 25°–35°; O: experimental data of J. B. Cladis, W. N. Hess, and B. J. Moyer, Phys. Rev. **87**, 425 (1952). The vertical scale for the experimental data is arbitrary.

to the $\pi^- + p$ cross section that was evaluated from experimental data.[11]

Pion absorption was accounted for in the same manner as before, that is, by assuming that the pion was absorbed by a two-nucleon cluster.[2] Pion absorption through the sequential reactions

$$\pi + N \rightarrow N^*,$$
$$N^* + N \rightarrow N + N$$

was not taken into account. A brief discussion of the reactions of isobars with nuclei is given in the next section.

PION PRODUCTION

Single- and double-pion-production events were assumed to take place through the formation of the $\frac{3}{2}$, $\frac{3}{2}$ isobar. The model employed was that of Sternheimer and Lindenbaum.[5] Double-pion production was restricted to nucleon-nucleon collisions where two such isobars were formed with subsequent decay. The $\frac{3}{2}$, $\frac{3}{2}$ isobar dominates the interactions even at the highest energies considered here.[12,13] Although the one-pion exchange model would serve adequately at the lower energies, it would be inappropriate at the higher energies.[12]

In single-pion-production events, the mass of the isobar was taken from the distribution

$$P(m, E) = k\sigma_{3/2}(m) F(m, E),$$

where m is the mass of the isobar, E is the relative kinetic energy of the incident pion or nucleon, k is a normalization constant, $\sigma_{3/2}(m)$ is the total $\pi^+ + p$ cross section evaluated at the π^+ kinetic energy such that the total c.m. energy of the $\pi^+ + p$ system was m, and F is the phase space available to the isobar and recoil particle.

In double-pion production, the masses of the two isobars m_1 and m_2 were distributed as

$$P(m_1, m_2, E) = k\sigma_{3/2}(m_1)\sigma_{3/2}(m_2) F(m_1, m_2, E).$$

The upper limit of the available mass in each case was determined by the conservation of energy in each particle-particle reaction.

The lifetime of the $\frac{3}{2}$, $\frac{3}{2}$ isobar ($\sim 0.75 \times 10^{-23}$ sec), inferred from the width of the resonance, is such that interactions with other nucleons are possible before the isobar decays. In these interactions, the isobar can either scatter elastically, scatter inelastically and create other isobars, or it can react with a nucleon N such that $N^* + N \rightarrow N + N$. The latter reaction has been investigated by Fraenkel,[14] who calculated the cross section and estimated that the reaction would occur with a 40% probability in nuclear matter in comparison with isobar decay. If this is the case, the secondary-nucleon spec-

[11] V. G. Zinov and C. M. Korenchenko, Zh. Eksperim. i Teor. Fiz. **33**, 1307 (1957) [English transl.: Soviet Phys.—JETP **6**, 1006 (1958)]; L. K. Goodwin, R. W. Kenney, and V. Perez-Mendez, Phys. Rev. Letters **3**, 522 (1959); F. Grard, G. MacLeod, and L. Montanet, Nuovo Cimento **22**, 193 (1961); C. D. Wood *et al.*, Phys. Rev. Letters **6**, 481 (1961); B. C. Maglic *et al.*, Phys. Rev. **123**, 1444 (1961); R. C. Whitten and M. M. Block, *ibid.* **111**, 1676 (1958); K. W. Lai, L. W. Jones, and M. L. Perl, Phys. Rev. Letters **7**, 125 (1961).

[12] A. C. Melissinos *et al.*, Phys. Rev. **128**, 2373 (1962).

[13] G. Cocconi *et al.*, Phys. Letters **8**, 134 (1964).

[14] Zeev Fraenkel, Phys. Rev. **130**, 2407 (1963).

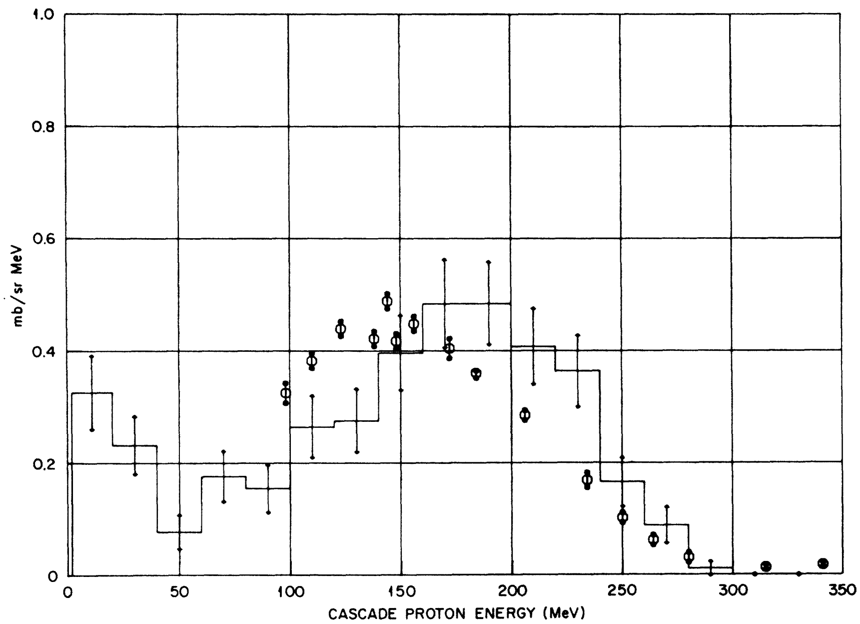

FIG. 14. Energy spectrum of cascade protons emitted at a laboratory angle of 40° from 340-MeV protons on carbon. Histogram: calculated values for the angular interval 35°–45°; O: experimental data, reference in Fig. 13. The vertical scale for the experimental data is arbitrary.

trum will be harder than if all the isobars decay. The isobar elastic and inelastic cross sections are not known. Some of the reactions of the isobars with the bound nucleons in the nucleus will be taken into account in calculations being performed elsewhere.[15] For simplicity, in the work reported here the isobar was assumed to decay at the space point where the collision occurred.

The angular distribution of the isobar in the c.m. system of the colliding particle was taken to be 50% isotropic, 25% forward, and 25% backward, and it was assumed to be energy-independent. The isobar was then made to decay isotropically in its own rest system. Secondary-nucleon spectra obtained using this angular distribution were indistinguishable from the spectra obtained using either a totally isotropic distribution or a distribution that was 50% forward and 50% backward. Isotropic decay of the isobar was assumed throughout. In every case, the trend in the data in going from totally

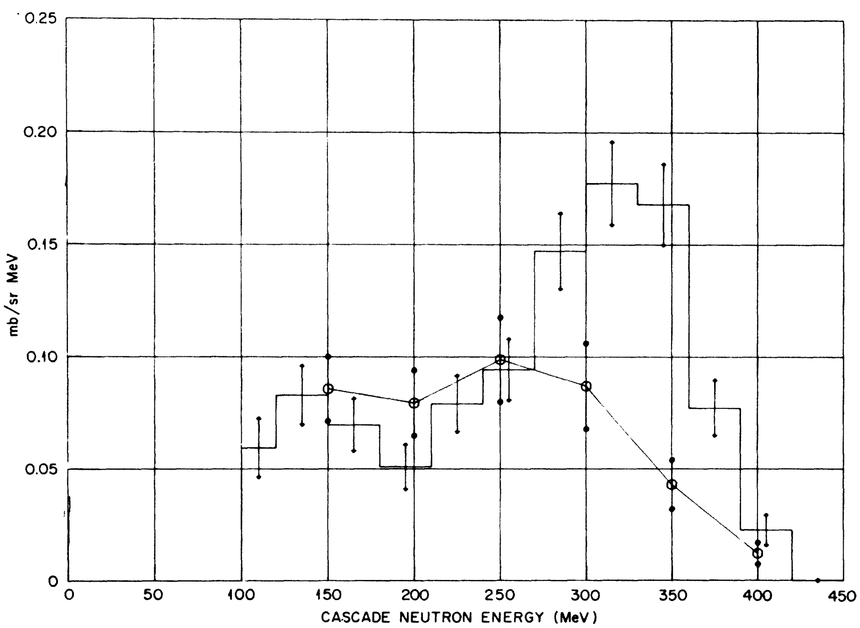

FIG. 15. Energy spectrum of cascade neutrons emitted at a laboratory angle of 30° from 450-MeV protons on carbon. Histogram: calculated values for the angular interval 25°–35°; O: experimental data of J. W. Wachter, W. A. Gibson, and W. R. Burrus, Ref. 19.

[15] J. M. Miller, Columbia University (private communication).

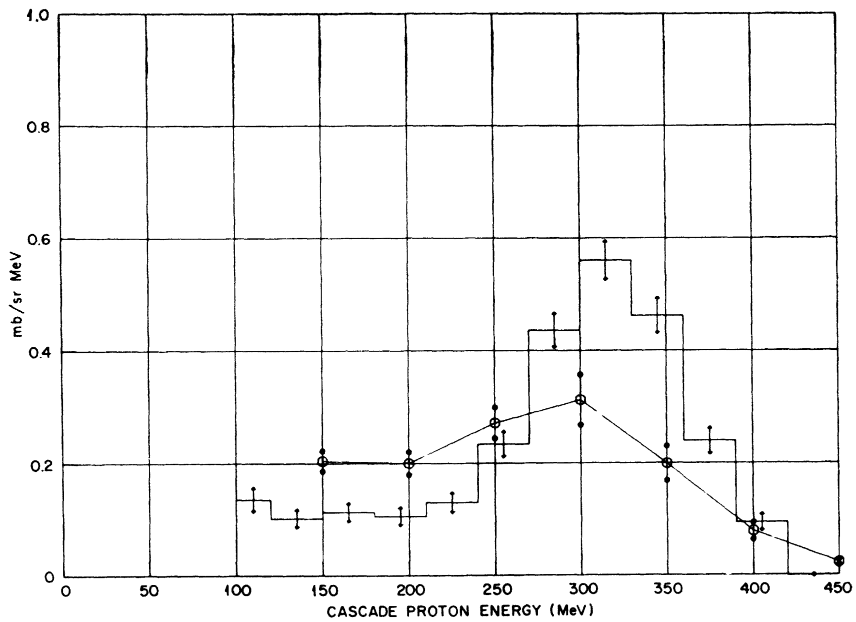

FIG. 16. Energy spectrum of cascade protons emitted at a laboratory angle of 30° from 450-MeV protons on carbon. Histogram: calculated values for the angular interval 25–°35°; O: experimental data, Ref. 19.

isotropic to the forward-backward distribution was masked by the statistics when the data from either one were compared with the data from the distribution chosen.

The charges of the particles in the final states for single-pion-production processes in *n-p* or *p-p* collisions are given by the Clebsch-Gordan coefficients within the framework of the isotopic spin formalism. For double-production processes, the ratio of the cross section for double production through the isotopic spin $T=0$ state to that for double production through the $T=1$ state had to be determined. This ratio was taken to be the same as that used to calculate the *n-p* double-production cross section.

For the pion-nucleon collisions leading to single production, the phase angle ϕ, between the matrix elements of the final isotopic spin states $T=\frac{3}{2}$ and $T=\frac{1}{2}$, and the ratio of the cross section for meson production through each of those final states must be known before the final charge states can be ascertained.[5] The quantity

$$\rho=\sigma_{\text{s.p.}}(T=\tfrac{3}{2})/2\sigma_{\text{s.p.}}(T=\tfrac{1}{2})$$

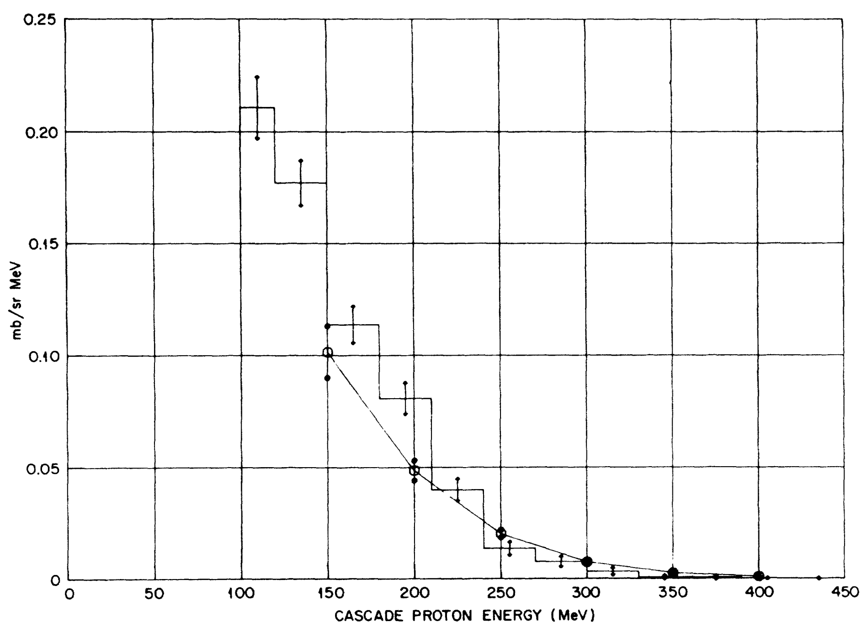

FIG. 17. Energy spectrum of cascade protons emitted at a laboratory angle of 60° from 450-MeV protons on carbon. Histogram: calculated values for the angular interval 50°–70°; O: experimental data, Ref. 19.

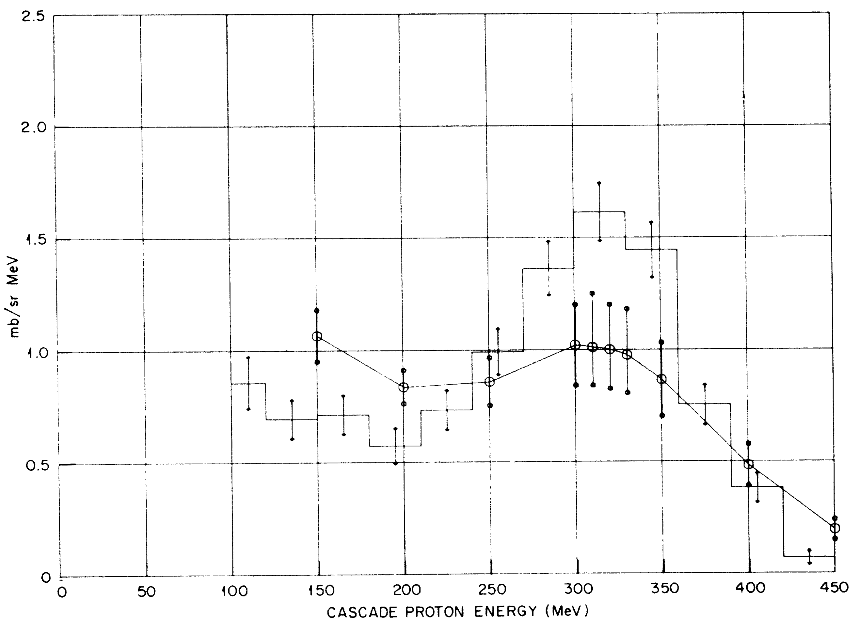

FIG. 18. Energy spectrum of cascade protons emitted at a laboratory angle of 30° from 450-MeV protons on bismuth. Histogram: calculated values for the angular interval 25°–35°; O: experimental data, Ref. 19.

was calculated from the expression

$$\sigma_{\text{s.p.}}(\pi^-+p)=\tfrac{2}{3}\sigma_{\text{s.p.}}(T=1)(1+\rho),$$

where $\sigma_{\text{s.p.}}(\pi^-+p)$ was assumed to be the inelastic π^-+p cross section, illustrated in Fig. 7, and $\sigma_{\text{s.p.}}(T=1)$ was taken to be the inelastic cross section for the $T=1$ isotopic spin state.[9] The phase angle ϕ was calculated from the expression

$$\sigma(\pi^-+p\rightarrow\pi^++\pi^-+n)=\tfrac{2}{3}\sigma_{\text{s.p.}}(T=1)\times[5/9+(26/45)\rho+(7/9)a],$$

where $a=2(\rho\frac{1}{5})^{1/2}\cos\phi$. The $\pi^-+p\rightarrow\pi^++\pi^-+n$ cross section that was used is shown in Fig. 8. It was assumed that the phase angle and ρ were the same for all charge combinations of the pion and nucleon.

A problem involving energy conservation is encountered when pions are created in the field of the nucleus if this field acts on the pions with the same strength as it does on the nucleons, as was assumed for this calculation. The problem arises because there are no provisions for the inclusion of potential energy in the relativistic equations governing the kinematics. Hence, the total energy (that is, the kinetic, potential, and

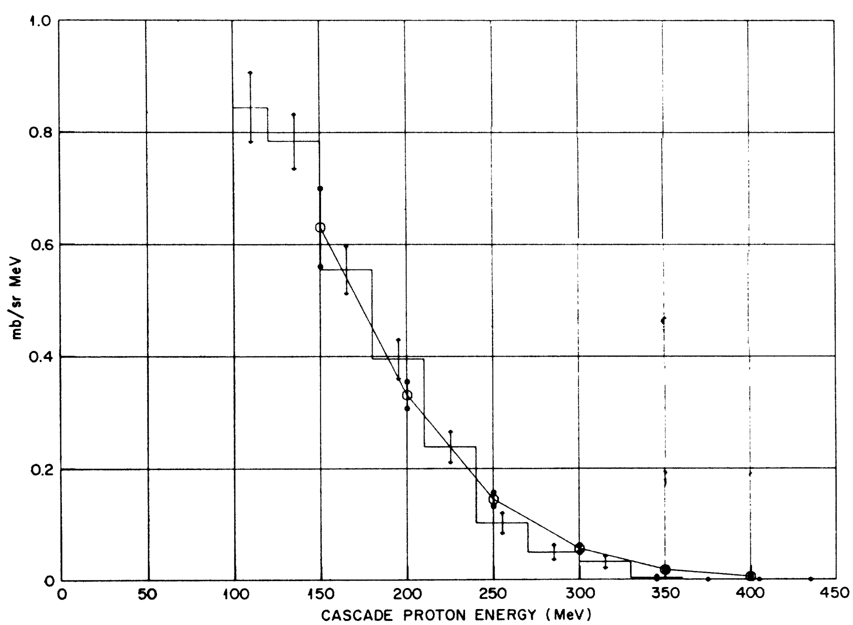

FIG. 19. Energy spectrum of cascade protons emitted at a laboratory angle of 60° from 450-MeV protons on bismuth. Histogram: calculated values for the angular interval 50°–70°; O: experimental data, Ref. 19.

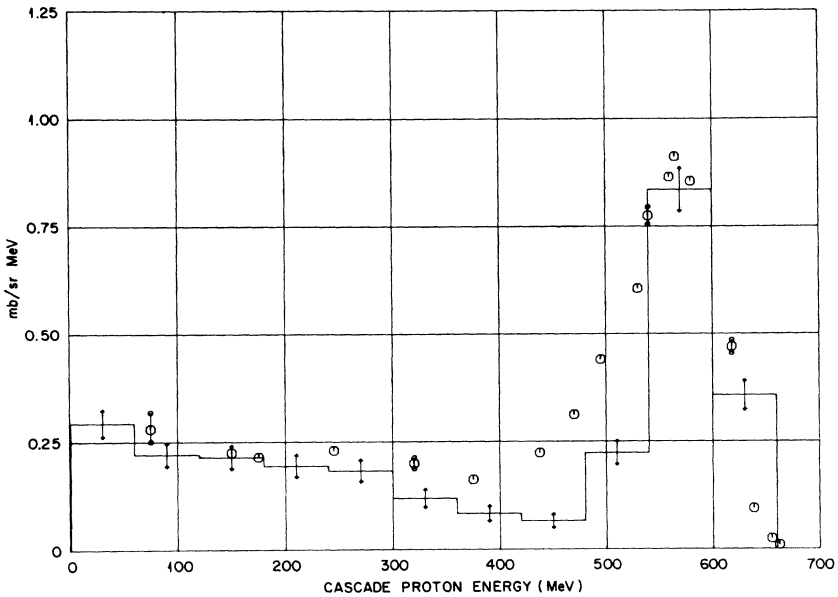

FIG. 20. Energy spectrum of protons emitted at a laboratory angle of 18° from 660-MeV protons on beryllium. Histogram: calculated values for the interval 13°–23°; circles: experimental data of L. S. Azhgirey *et al.*, Ref. 20.

mass energy) changes as the number of particles affected by the potential changes during the interaction. To circumvent this difficulty, the kinetic energies of the decay products of the isobar were arbitrarily increased by an amount required to conserve total energy. These energy increases were about half the depth of the nuclear potential in the region where the collision occurred.

COMPARISON WITH PREVIOUS CALCULATION

As mentioned above, the main differences between the earlier work[1,4] and that reported here are that in this work a pion-production model more representative of the free-particle data and a more realistic nuclear model were used. In attempting to determine the differences in the results that might be caused by these changes, comparisons were made with an angular distribution, an energy spectrum, and some of the nucleon multiplicities published previously. Data were calculated both for a constant-density nucleus of the same radius as that used by Metropolis *et al.*[1,4] and with the diffuseness of the nuclear surface taken into account. Therefore, in comparison with the data of Metropolis *et al.*, differences in the results where the same nuclear sizes and densities were used are presumably due to the pion-production model. However, definitive conclusions in

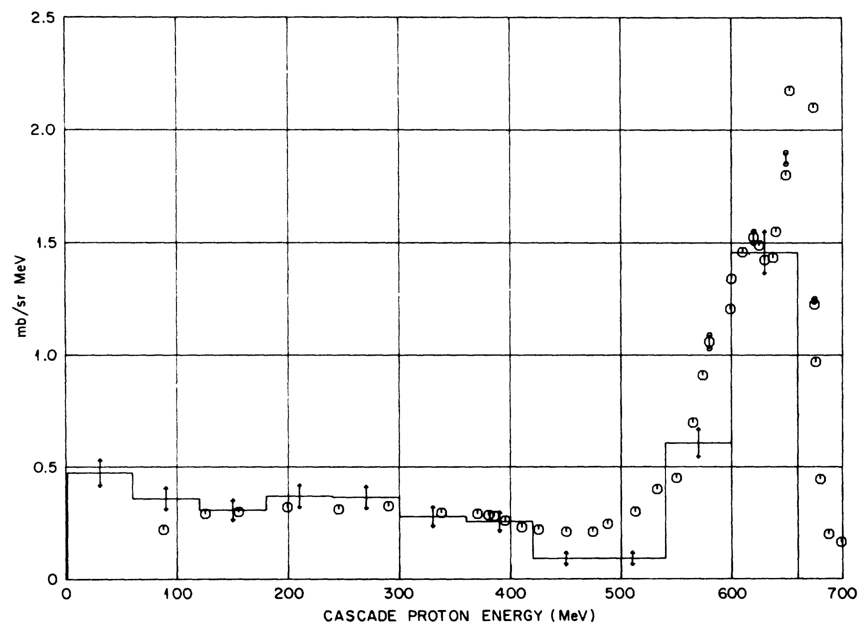

FIG. 21. Energy spectrum of protons emitted at a laboratory angle of 12.2° from 660-MeV protons on carbon. Histogram: calculated values for cascade protons emitted in the angular interval 7°–17°; ○: experimental data, Ref. 20. The largest values of the experimental spectra at the elastic peak are not illustrated.

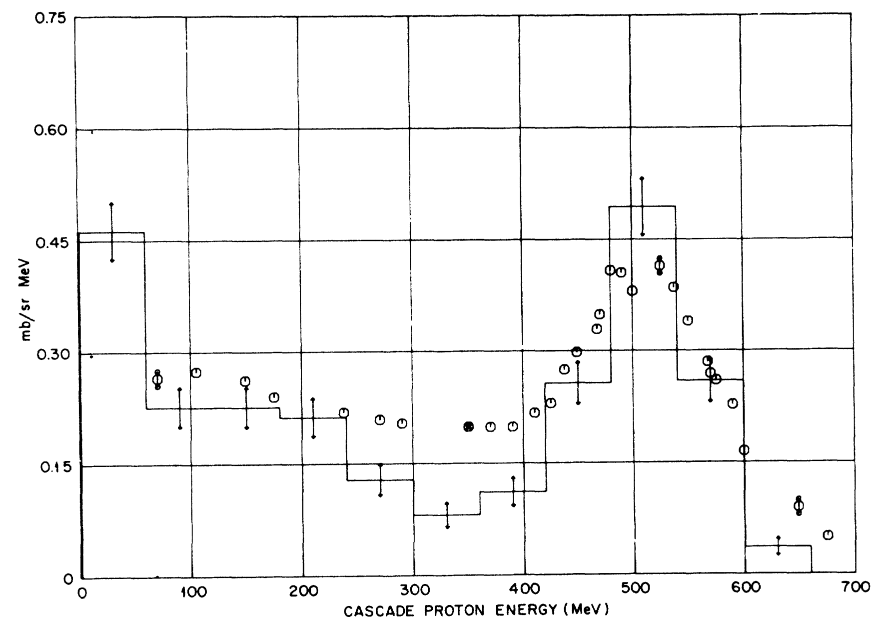

FIG. 22. Energy spectrum of cascade protons emitted at a laboratory angle of 24° from 660-MeV protons on carbon. Histogram: calculated values for the angular interval 20°–30°; ○: experimental data, Ref. 20.

this regard are obscured by the fact that somewhat different elementary-particle cross sections were used and the fact that a completely different sampling technique was employed for determining the momentum and the type of struck particle, as well as the kind of reaction with this particle. Taking these facts into consideration, the comparisons that were made are illustrated in Tables II and III and in Figs. 9 and 10.

The angular distribution of Metropolis *et al.*[4] for 1840-MeV protons on aluminum shown in Fig. 9 is not quite as peaked forward as the two distributions from the present calculation.

The neutron-to-proton ratio in Table II in the case of the copper target for the same nuclear configuration as that of Metropolis *et al.* shows a significant difference from their data. The effect of the diffuse edge appears to decrease the average number of emitted nucleons, as shown in Table III, but they are emitted with greater energy, as is illustrated by the high-energy peak in the spectrum in Fig. 10.

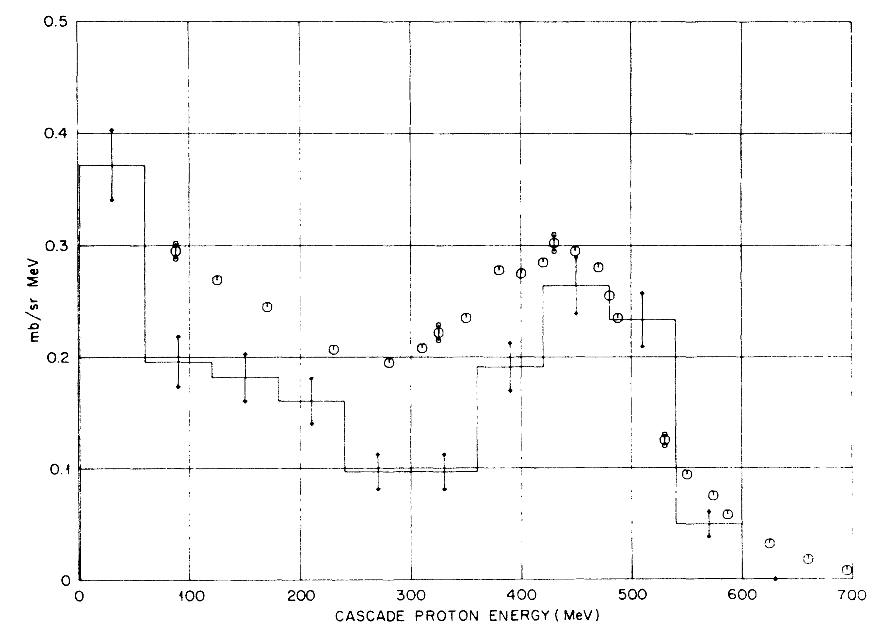

FIG. 23. Energy spectrum of cascade protons emitted at a laboratory angle of 30° from 660-MeV protons on carbon. Histogram: calculated values for the angular interval 25°–35°; ○: experimental data, Ref. 20.

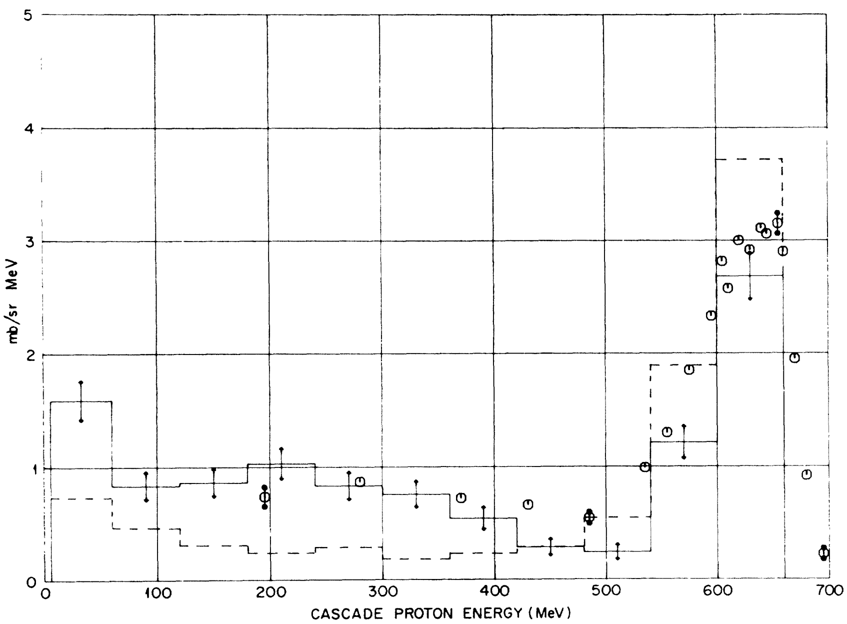

FIG. 24. Energy spectrum of protons emitted at a laboratory angle of 12.2° from 660-MeV protons on copper. Solid-line histogram: calculated values for the angular interval 7°–17° with pion production included; dashed-line histogram: calculated values without pion production for the interval 6°–18°; O: experimental data, Ref. 20.

COMPARISON WITH EXPERIMENT

Total Nonelastic Cross Sections

The theoretical and experimental nonelastic cross sections as a function of energy for protons and neutrons on several nuclei are given in Figs. 11 and 12. In general, the predicted cross sections lie within the bounds of the somewhat erratic energy-dependent behavior obtained from the experimental points. However, the calculated cross sections for protons on carbon appear to be consistently larger by about 5–15%, while the overestimate for incident neutrons reaches 30%. This may be attributed to the fact that the constants in the Fermi-type charge distribution function deduced by Hofstadter[6] for other elements cannot be directly applied to a light, tightly bound nucleus such as carbon; that is, the diameter of such a nucleus used in the theoretical model may be too large.

Other than this, the agreement between the experimental data and theoretical predictions is reasonable.

Secondary-Nucleon Spectra

The following comparisons of the secondary nucleon spectra with experiment are arranged according to the

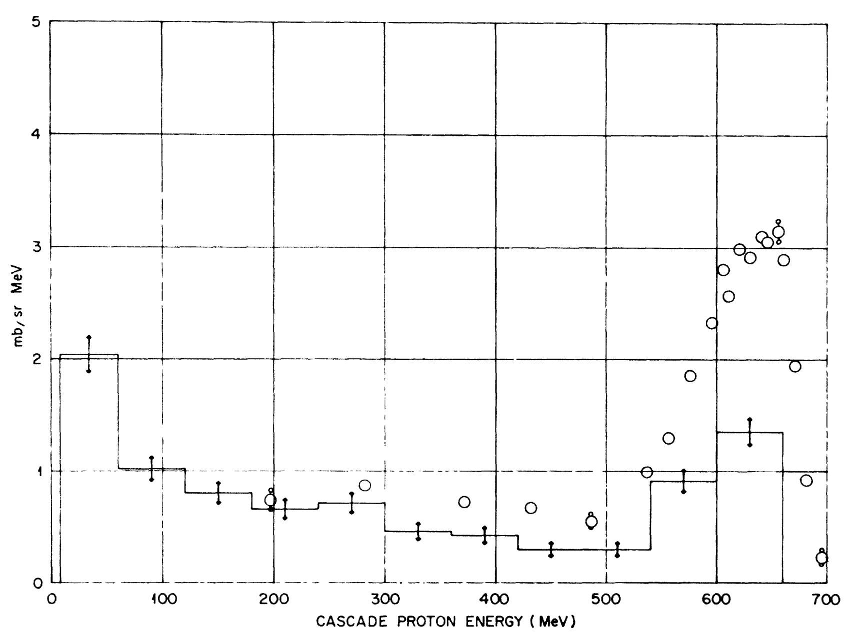

FIG. 25. Same spectral case as in Fig. 24. Histogram: calculated values for the angular interval 7°–17° using the same nuclear size and density as Metropolis *et al.* (Ref. 1); O: experimental data same as Fig. 24.

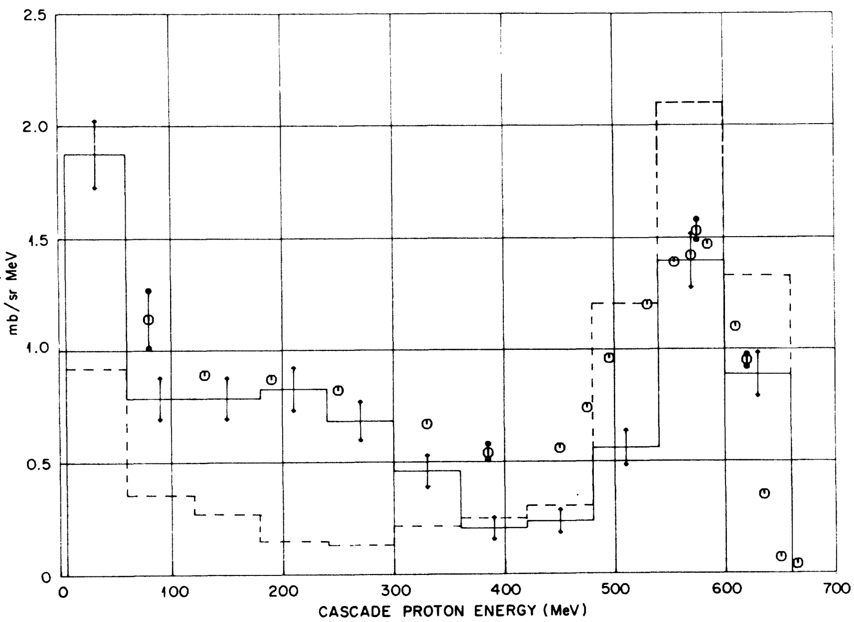

FIG. 26. Energy spectum of cascade protons emitted at a laboratory angle of 18° from 660-MeV protons on copper. Same notation as in Fig. 24. The angular interval used for the calculated data is 13°–23°.

increasing energy of the incident particle. Many comparisons have been made that are not presented in this paper, but they are published elsewhere.[16] Since neither elastic scattering nor the discrete eigenstates of the nucleus in the final state are included in the theory, the comparisons with experiment are valid only in the quasifree region of the spectra.

All predictions are in absolute units, and all but the first two comparisons are on an absolute basis. In the first two cases, the experimental data were reported in relative units. One of the strongest points of the present theoretical approach is that there are no parameters to adjust in the calculation in the sense that one must rely on the results of particle-nucleus experiments to determine these parameters. The unknowns that do exist are those pertaining to the free-particle reactions or those that refer to the nuclear density distribution. The unknowns related to the elementary cross sections are determined from the experimental free-particle reactions or from basic symmetry principles such as the

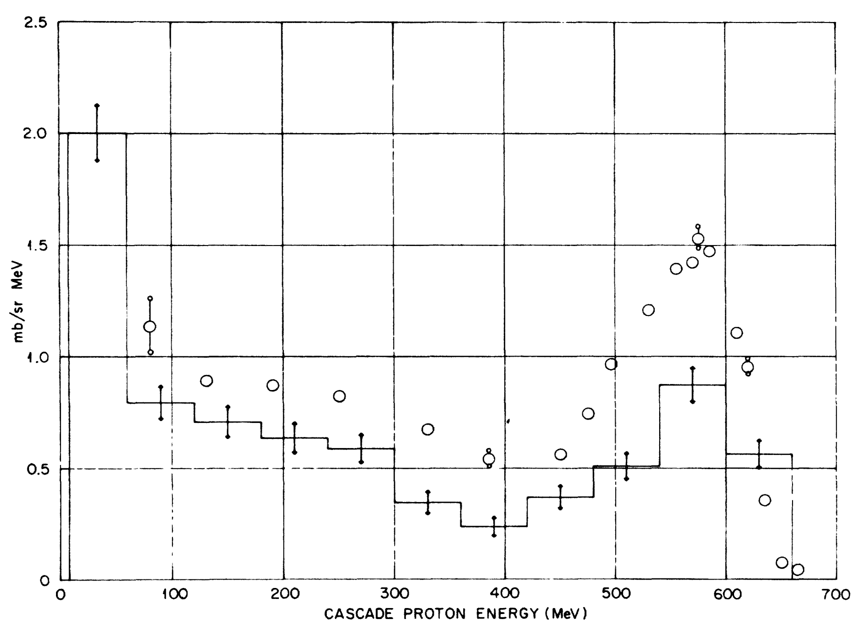

FIG. 27. Same spectral case as in Fig. 26. Histogram: calculated values for the angular interval 13°–23° using the same nuclear size and density as Metropolis *et al.* (Ref. 1); ○: experimental data same as Fig. 26.

[16] H. W. Bertini, A. H. Culkowski, and M. P. Guthrie, Oak Ridge National Laboratory Report No. ORNL-TM-2361, 1969 unpublished).

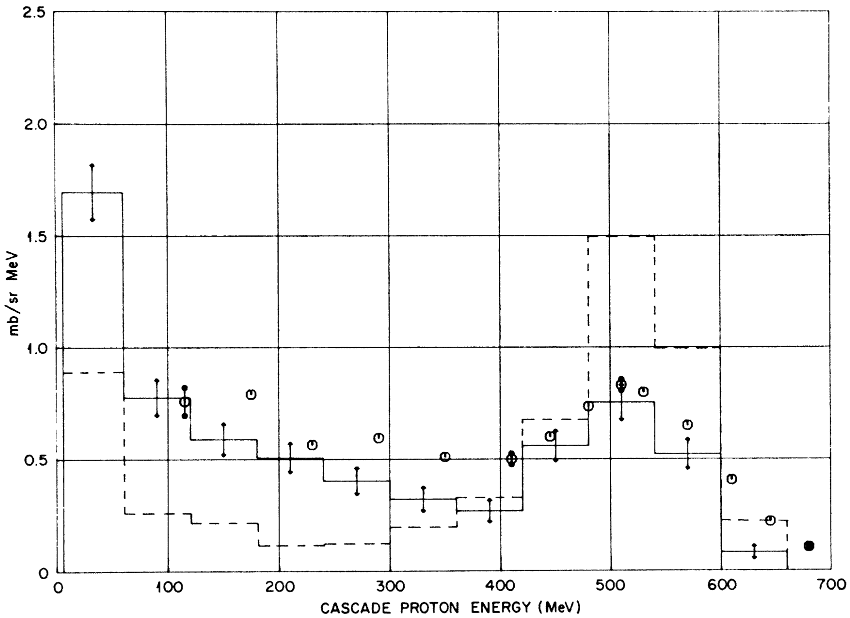

FIG. 28. Energy spectrum of cascade protons emitted at a laboratory angle of 24° from 660-MeV protons on copper. Same notation as in Fig. 24. The angular interval used for the calculated data where pion production is included was 20°–30°, while for calculation without pion production it was 19°–29°.

conservation of isotopic spin, while the nuclear-density distribution is determined from the electron scattering data.[6]

Figures 13 and 14 illustrate the secondary proton spectra at 30° and 40° from 340-MeV protons on carbon. The experimental data have been normalized to the results of the calculation. At 30° the theoretical peak is somewhat sharper than that from the experiment.[17] At 40° the shapes of the spectra are in reasonable agreement, but the position of the experimental peak is at a lower value than the predicted one. This discrepancy cannot be totally attributed to the binding energy of the recoil nucleon that is likely to be emitted in these quasifree reactions.[17] Other theoretical approaches lead to the same discrepancy.[18]

Figures 15 and 16 illustrate comparisons made with the experimental neutron and proton spectra at 30° from 450-MeV protons on carbon. The pronounced

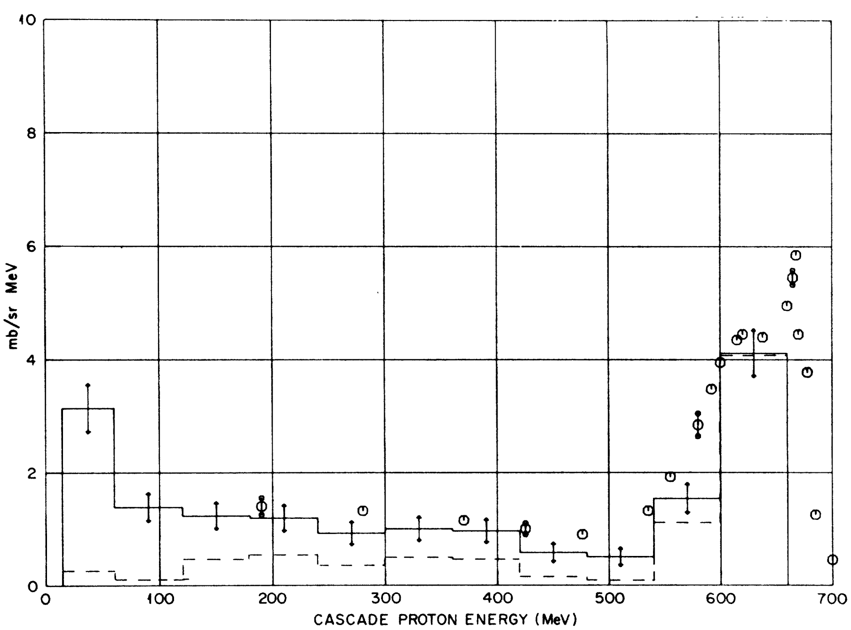

FIG. 29. Energy spectrum of cascade protons emitted at a laboratory angle of 12.2° from 660-MeV protons on uranium, Solid-line histogram: calculated results where all particles excaping into angular interval 7°–17° contribute; dashed-line histogram: theoretical spectrum resulting from the contributions of single-collision reactions only; O: experimental data, Ref. 20.

[17] J. B. Cladis, W. N. Hess, and B. J. Moyer, Phys. Rev. **87**, 425 (1952).
[18] Peter A. Wolff, Phys. Rev. **87**, 434 (1952).

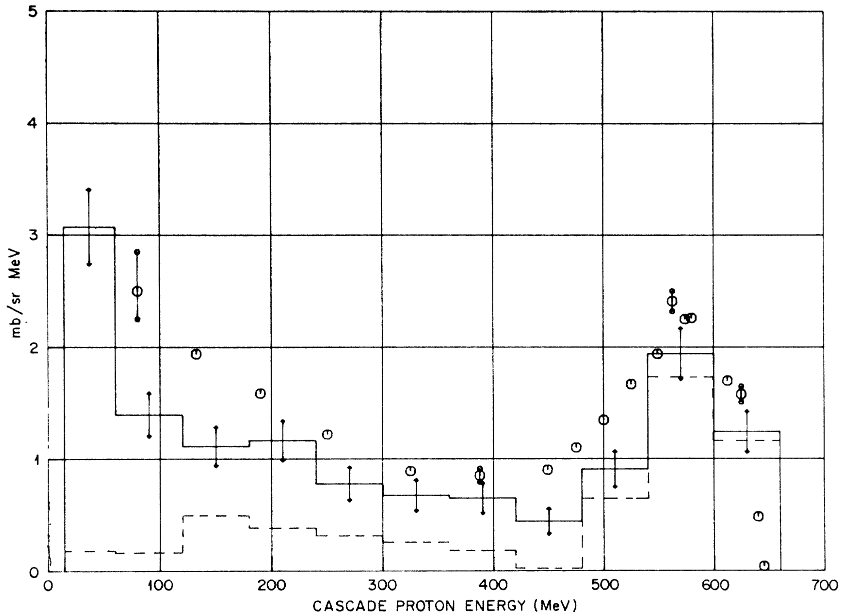

Fig. 30. Energy spectrum of cascade protons emitted at a laboratory angle of 18° from 660-MeV protons on uranium. Same notation as in Fig. 29. The angular interval used for the calculated data was 13°–23°.

quasifree peaks that are predicted by the calculation are not manifest in the experimental data,[19] which yield bumps rather than peaks. At wider angles the agreement is better, as is shown in Fig. 17. These comparisons are typical when other light elements were used in the 450-MeV experiments. The discrepancy shown in Fig. 15 persists in the neutron spectrum from a cobalt target. The bump in the experimental proton spectrum at 30° shifts to somewhat higher energies as the target mass is increased, which enhances the agreement with the predictions, and the agreement between theory and experiment at all angles for a bismuth target, illustrated for two angles in Figs. 18 and 19, is improved.

Figures 20–31 contain comparisons between theory and experiment[20] of the secondary-proton spectra from 660-MeV protons on four elements: beryllium, carbon, copper, and uranium. An example of the comparisons for a beryllium target is shown in Fig. 20. The agree-

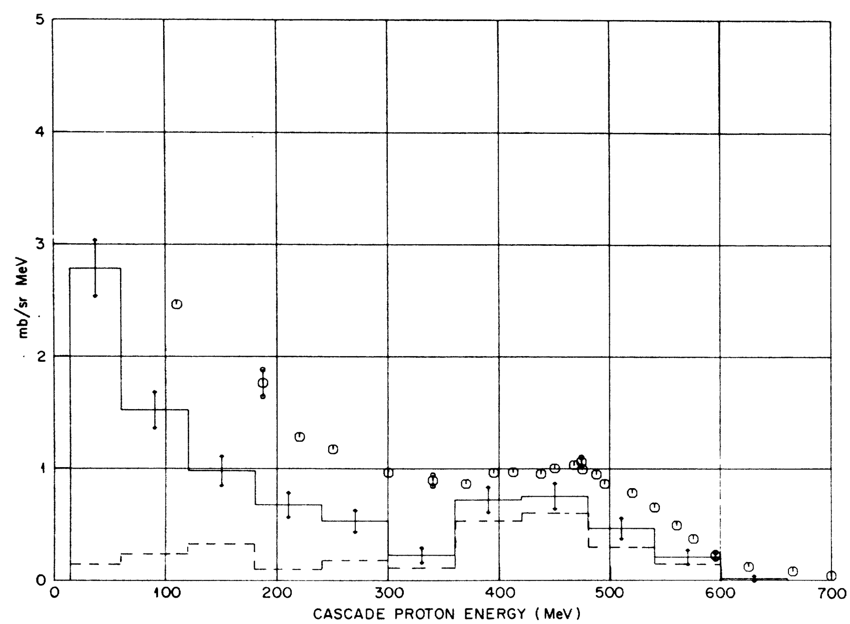

Fig. 31. Energy spectrum of cascade protons emitted at a laboratory angle of 30° from 660-MeV protons on uranium. Same notation as in Fig. 29. The angular interval used for the calculated data was 25°–35°.

[19] J. W. Wachter, W. A. Gibson, and W. R. Burrus, Oak Ridge National Laboratory Report No. ORNL-TM-2253, 1968 (unpublished).

[20] L. S. Azhgirey, I. K. Vzorov, V. P. Zrelov, M. G. Mescheryakov, B. S. Neganov, R. M. Ryndin, and A. F. Shabudin, Nucl. Phys. **13**, 258 (1959).

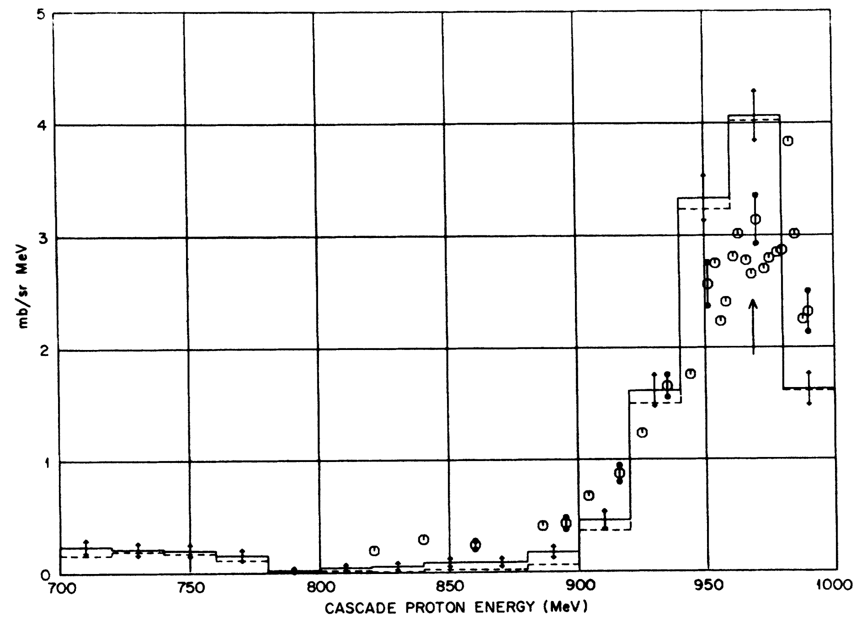

FIG. 32. Energy spectrum of cascade protons emitted at a laboratory angle of 9.1° from 1-GeV protons on carbon. Solid-line histogram: calculated results for the angular interval 7°–11°; O: experimental data of Corley and Wall (Ref. 21). The location of the experimental quasifree peak was determined by Corley and Wall and is indicated by the arrow. Dashed-line histogram: theoretical spectrum resulting from the contribution of single-collision reactions only. The angular interval used was the same as for the solid-line histogram.

ment is quite good. Figures 21–23 show comparisons for a carbon target. At 12.2° (Fig. 21), the shoulder in the experimental data at about 620 MeV is attributed to the quasifree peak.[20] The experimental data at energies greater than 620 MeV are due to elastic scattering[20] which is not included in the calculation. At the other angles, there is no contribution from elastic scattering. With the exception of the data at the widest angle (Fig. 23), the agreement over the entire range of measured secondary-proton energies is quite good. Even at the widest angle 30°, the shape of the theoretical spectrum is in reasonable agreement with the experimental data, but the magnitude of the predicted spectrum falls below that of the measured one. This is rather typical of the comparisons of all the elements at this angle for 660-MeV incident protons.

The effect of pion production and the effect of the diffuse nuclear surface on the comparisons with the experimental data for a copper target are shown in Figs. 24–28. When pion production is eliminated, the resulting spectra are illustrated by the dashed lines in Figs. 24, 26, and 28. The quasifree peaks are too high,

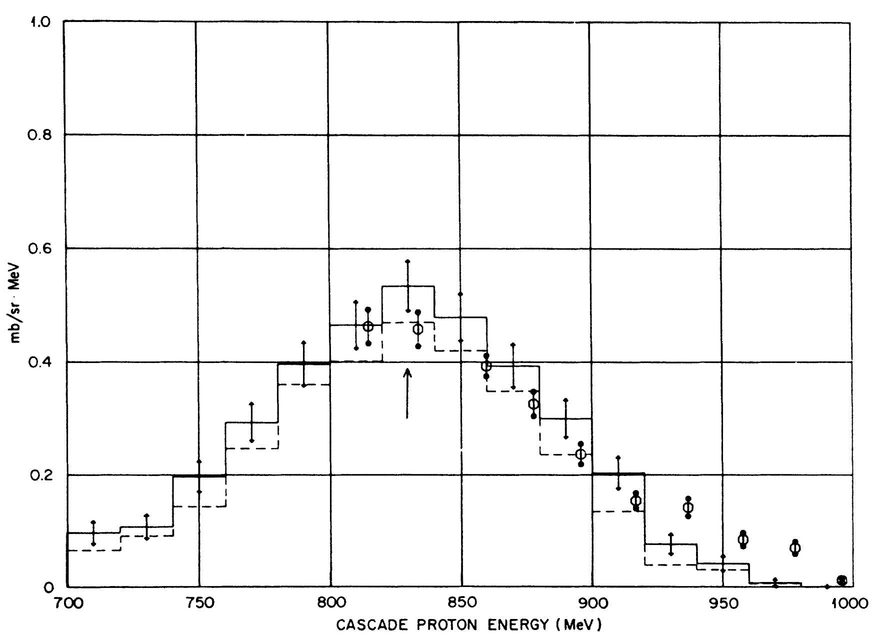

FIG. 33. Energy spectrum of cascade protons emitted at 20.2° from 1-GeV protons on carbon. Symbols are described in Fig. 32. The angular interval used in the calculation of both theoretical spectra was 17°–23°.

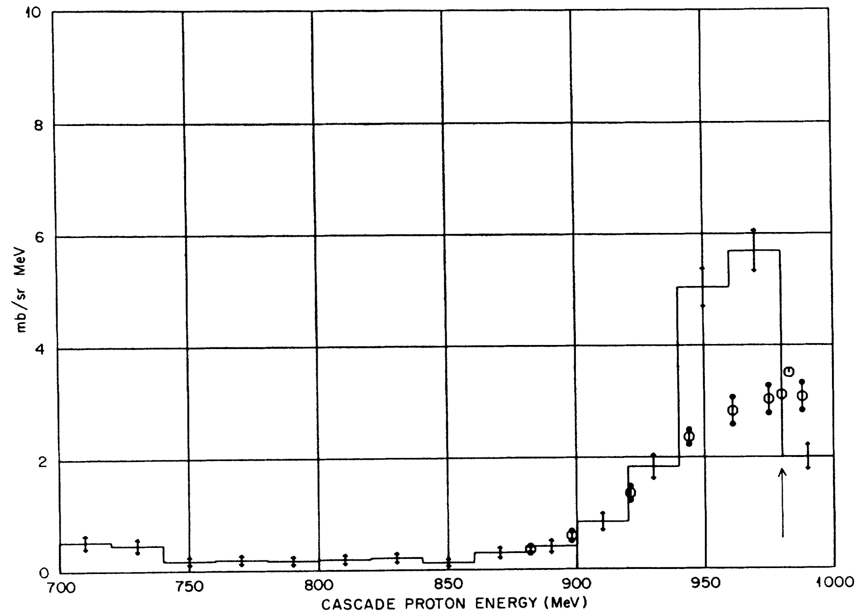

FIG. 34. Energy spectrum of cascade protons emitted at a laboratory angle of 9.15° from 1-GeV protons on calcium. Symbols are described in Fig. 32. The angular interval used in the calculation was 7°–11°.

and the values of the spectra at the lower energies are too small. The small differences that were sometimes used in the angular intervals of the theoretical calculations with and without pion production have no significance. Figures 25 and 27 illustrate the results obtained when the diffuse nuclear surface is eliminated, and a nucleus of the same configuration as Metropolis *et al.*[1,4] is used, that is, a nucleus with a constant nucleon density throughout and a radius given by $r=1.3A^{1/3}$ F. The predicted quasifree peaks are too small. This illustrates the importance of the diffuse boundary in these reactions. Without it, the very good agreement with experiment that is illustrated in Figs. 24, 26, and 28 could not have been achieved.

Comparisons between theoretical results and experimental data for 660-MeV protons on uranium are shown in Figs. 29–31. The agreement at all but the widest angle is quite good. At the widest angle, the predicted spectrum is typically lower than the measured one.

The dashed-line histograms in these figures show the contribution to the spectra of escaping protons that are either knocked out or scattered out without subsequently colliding when the incident proton makes its first collision inside the nucleus. These single-scattering contributions dominate the spectra in the vicinity of the quasifree peaks, which is rather interesting because the target is a very heavy element.

At higher energies, comparisons for 1000-MeV protons on carbon and calcium are illustrated in Figs. 32–35. The calculated quasifree peaks are generally sharper than the measured ones,[21] but the positions of the peaks are in reasonable agreement. The large arrows in these figures indicate the positions at which Corley and Wall locate the experimental peaks. The spectra from single-scattering events, shown in Figs. 32 and 33, again dominate the spectra in the quasifree region. It is interesting to note that the spectra from single-scattering events are not greatly distorted from those in which all events contribute. There are even significant contributions to the wings of the spectra—a result that was not anticipated.[21] The dominant role played by the single-scattering events in the high region of the spectra is to be expected for light elements.

The last comparison is shown in Fig. 36, in which the calculated and experimental data at the low-energy end of the proton spectrum at forward angles are illustrated. The reaction is 2.7-GeV protons on heavy emulsion nuclei. The agreement is very good. The lowest-energy points of the data of Piroué and Smith[22] are not illustrated because the data at these energies are greatly affected by target absorption.[23] The calculated and experimental angular distributions of the secondary protons for the same reaction, shown in Fig. 1 of the following article,[24] are in good agreement.

The comparisons at 2.7 GeV are at an energy where triple-pion production may be important, and hence the calculation is being applied where its validity is questionable. Furthermore, the momenta of the struck nucleons in the calculation are restricted to those values for which the relative kinetic energy between the incident and struck nucleon is less than 3.5 GeV—the maximum value for which cross sections are tabulated. In other words, the incident particle is not permitted to interact

[21] Daniel M. Corley, Ph.D. thesis, University of Maryland, 1968 (unpublished).

[22] P. A. Piroué and A. J. S. Smith, Phys. Rev. **148**, 1315 (1966).

[23] P. A. Piroué (private communication).

[24] D. T. King, following paper, Phys. Rev. **188**, 1731 (1969).

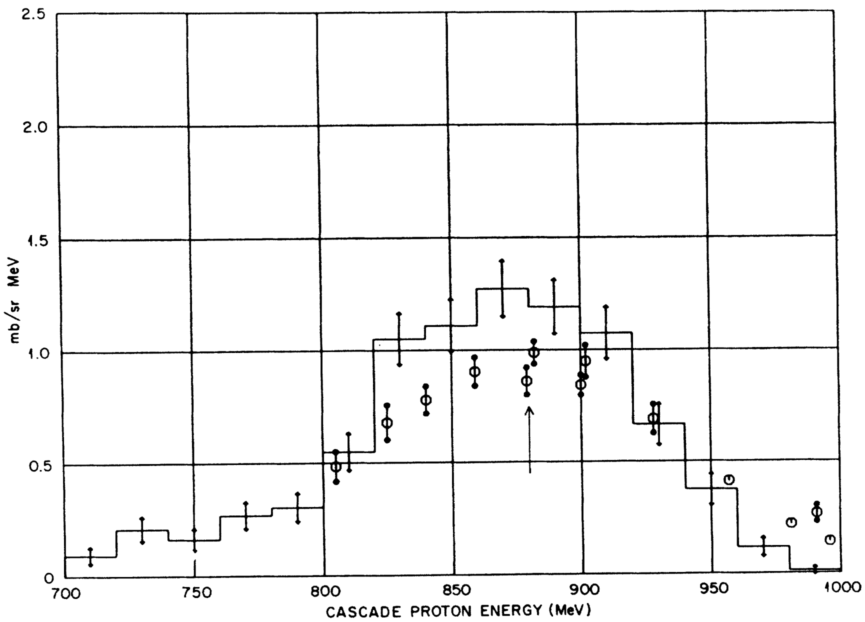

FIG. 35. Energy spectrum of cascade protons emitted at a laboratory angle of 17.2° from 1-GeV protons on calcium. Symbols are described in Fig. 32. The angular interval used in the calculation was 15°–19°.

with those bound nucleons near the top of the Fermi sea whose vector momenta are directed toward the incoming particle. The two approximations at these energies (that is, ignoring triple- and higher multiple-pion production, and sampling from a distorted struck-particle distribution) may not be important for these particular comparisons, which apply to escaping nucleons only—and one can see why. In the calculation, the sum of the scattering, single-production, and double-production cross sections that were used at any energy is essentially equal to, and sometimes exceeds, the measured total cross section at that energy. Since triple production is being ignored and the greatest uncertainties lie in the determination of the single- and double-production cross sections, then it can be assumed that triple production is very likely being replaced by either single or double production in the calculation. Hence, the effect of producing one or two pions in place of producing three pions occasionally should not greatly distort the low-energy nucleon spectra.

The distortion that is introduced in sampling from

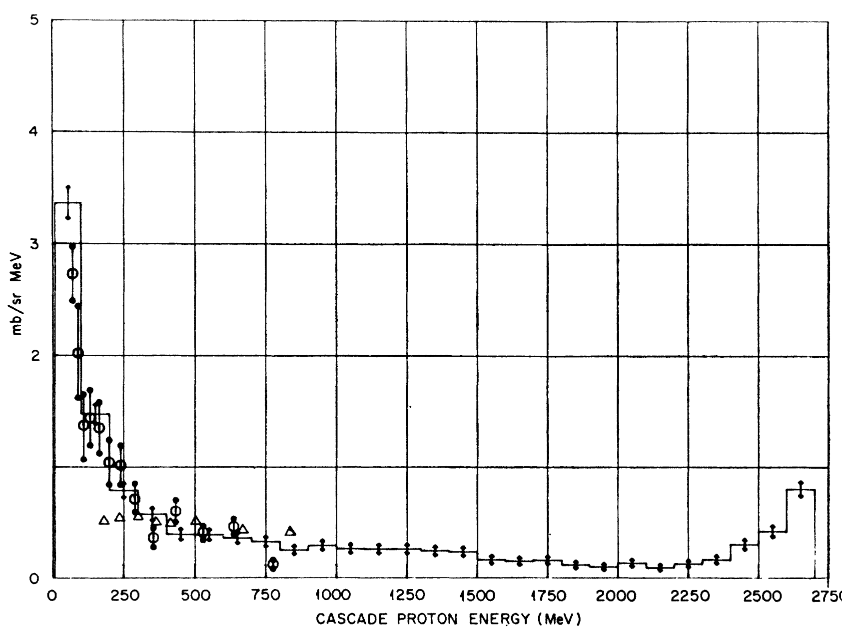

FIG. 36. Energy spectra of cascade protons emitted in the angular interval 0–30° from 2.7-GeV protons on heavy emulsion nuclei. ○: experimental data from D. T. King (Ref. 24); △: experimental data of P. A. Piroué and A. J. S. Smith (Ref. 22) for secondary protons emitted at 13° from 2.9-GeV protons on platinum; histogram: calculated values for a ^{100}Ru target averaged over the angular interval 0°–30°.

the struck-particle distribution is confined to a relatively small region of struck-particle-momentum space, but it is a region in which the colliding particles have the greatest relative kinetic energy. Since the pion multiplicity does not appear to be strongly energy-dependent,[25] the over-all effect on the nucleon spectra under consideration is again probably small.

CONCLUSIONS

The intranuclear-cascade model that describes the continuum-state interactions of 300–3000-MeV nucleons with complex nuclei gives a resonably accurate description of the secondary-nucleon spectra. The model is essentially free of parameters, and hence continuum-state interaction cross sections over broad energy ranges and target masses can be calculated on an absolute basis.

Experimental evidence for the existence of peaks in the energy regions of the secondary-particle spectra corresponding to continuum-state transitions exists in the energy range 340–1000 MeV. Both the positions and magnitude of these peaks are predicted rather well by the model, although the calculated peaks are, in general, somewhat sharper than the experimental peaks at forward angles. Indications are that the peaks are dominated by single-scattering or quasifree-scattering events for both light- and heavy-weight elements.

In contrast to the spectra obtained when the diffuseness of the nuclear boundary is taken into account, the values of the quasifree peaks are too small when the nuclear density is assumed to be constant and when the radius is taken to be $r=1.3A^{1/3}$ F.

Pion production reduces the size of the high-energy peaks and enhances the values of the spectra at the lower energies.

[25] G. Cocconi, L. J. Koester, and D. H. Perkins, in the Proceedings of the High Energy Physics Study Seminars, No. 28, Part 2, UCID 1444, 1961 (unpublished).

ACKNOWLEDGMENTS

A calculation of this complexity could not have been completed in a reasonable time by one person. The author gratefully acknowledges the competent assistance of Mrs. Arline Culkowski, who did the computer programming, Mrs. Miriam P. Guthrie, who assisted in the assimilation of the myriad of details and in the over-all checking, and Mrs. Elsie Pickell, Miss Barbara Bishop, and Mrs. Jackie Gillen for the countless hand computations that were required to reduce the experimental free-particle data to useful input.

APPENDIX: PROGRAM INFORMATION

The calculation is programmed in FORTRAN with a few of the subroutines in FAP. It operates on the IBM-7090 computer. The maximum number of incident-particle histories that were followed in generating the spectral data for this report was 50 000 for the case of 1-GeV protons on carbon, while the minimum was 5000 for 2.7-GeV protons on ruthenium. For both the cascade and editing codes, the running time for the carbon case was about 20 min, while for ruthenium it was 5 h. The running time is dependent on the mass of the target, and it is also very sensitive to the cutoff energy. For example, in the case of 2700-MeV protons on ruthenium (Fig. 36) using the standard Coulomb-barrier cutoff energy, it took about 5 h to follow the histories of 5000 incident particles. When the same case was rerun with a 100-MeV cutoff energy, it took $\frac{1}{2}$ h. This is due to the increased number of collisions that the low-energy particles undergo, which generates more cascade particles whose histories must be traced, and it is also due to the inefficiency of the sampling techniques when the cross sections are varying rapidly with energy, which they do at low energy.

The program will not be available for general use until the new particle-particle cross-section data have been incorporated.[10]